White Paper XXXIII

What Might a Phase-Transformation "Analog-Model" Teach Us About Our Global Autism IHD Broadcasting Experiment?

by

W. A. Tiller, Ph.D.

A. A General pathway to scientific understanding of a new technical area [1]

Reference 1 provides a complete and sufficient description of this topic for any serious reader as a "primer" for IHD applications to information medicine.

For example, there are two basic ways of approaching crystal growth phenomena. The first is the time-honored method of enquiry which treats the phenomenon as a "black box" whose internal characteristics are unknown, but are amenable to probing and analysis. Such a situation always occurs in the early stages of development of any new field of knowledge and is illustrated in Figure 1a. Here, we apply some input stimulus (IS) to the box and determine some output response (OR). By correlating the OR with the IS, we eventually deduce valuable information about the most probable internal behavior of the box for this degree of stimulus.

Experiments carried out over time usually allows one to discriminate the various coupled processes operating in the black box that generate such an "OR" spectrum as we vary (IS). This allows us to move to the Figure 1b stage of development of a systems approach, a more science-based approach, to investigating the phenomenon.
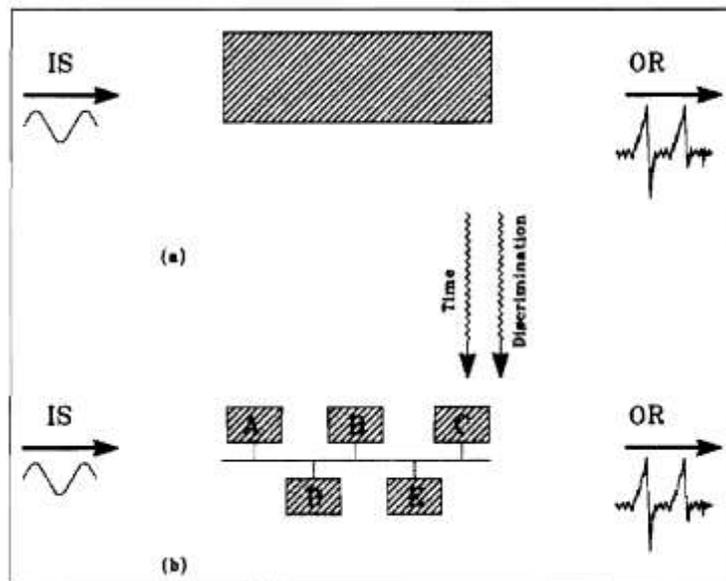
Figure 1. Schematic illustration of the "black box" metaphor (top) as a time-honored procedure for gaining sufficient understanding of a new phenomenon to recognize it as an interacting system of discriminated pieces of basic physics and chemistry (bottom)
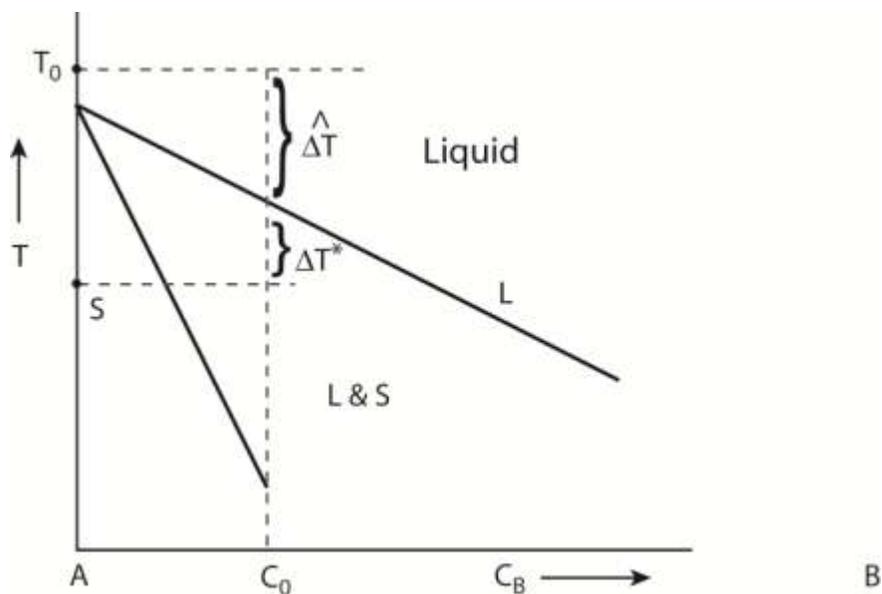

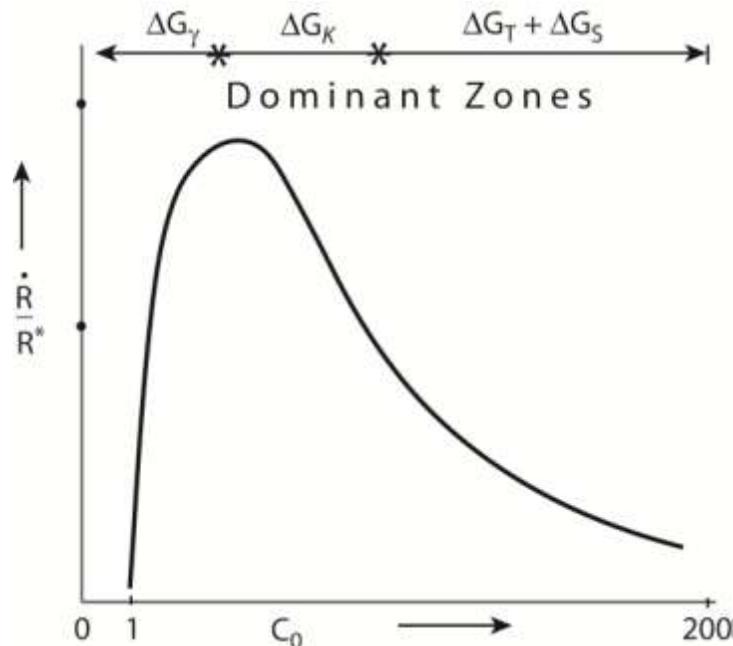Figure 2. Binary phase diagram for an alloy melt of composition, C_O, that is an initially superheated by an amount $\widehat{\Delta T}$.

Figure 3. Relative crystal velocity, Ṙ/R* vs. relative crystal size, R/R*

To illustrate this procedure, let us consider the simple case of a binary alloy liquid of major Constituent A and alloying Element B, as illustrated in Figure 2. This temperature, T-composition, C_B, diagram defines the thermodynamic equilibrium phase boundaries for the experimental variables (T,C_B). In the region of (T, C_B) **above** the liquidus line, L, any value of temperature and concentration, C_B, is thermodynamically stable so no change occurs. In the region of (T, C_B) **below** the solidus, line, S, any value of temperature and concentration, C_B, is thermodynamically stable. In the region of (T, C_B) **between** the liquidus and solidus lines, L+S, a **mixture** of both solid (crystals) and liquid is thermodynamically stable with the volume ratio of the two **totally determined** by the average temperature of the system. Now let us consider the actual **crystal growth process** itself.

Let us consider the case where we start our dynamic process of cooling and evaporation of Element A from that particular body of liquid defined by (T_o,C_0), where C_0 is the initial concentration of Component B. If the evaporation rate was zero and the average cooling rate for this fluid volume was $\dot{T}$, then the average thermodynamic state of this liquid volume as a function of time it would be (T_o- $\dot{T}t$,C_0); this fluid volume condition would eventually vertically penetrate the liquidus line, and would begin to become **thermodynamically unstable** with respect of the formation of solid (it is now **possible** for crystal growth to occur).

If, on the other hand, the cooling rate, $\dot{T}$, was zero ($\dot{T}$=o, so T(t)=T_o) and the average evaporation rate of Element A was $\dot{C}_A$, then the thermodynamic state of our initial liquid volume would change over time t_o (T_0, -C_0+$\dot{C}_A$t) and would move horizontally to remain in a thermodynamically stable liquid domain and no driving force for solid (crystals) exists.

In nature, we may have both average cooling at rate, $\dot{T}$, and average evaporation at rate, $\dot{C}_A$, occurring simultaneously so our initial volume of liquid, over time, t, changes its thermodynamic state diagonally to (To-$\dot{T}t$, C_0+$\dot{C}_A$t) and, depending upon the relative magnitudes of $\dot{T}$ and $\dot{C}_A$ plus the **actual slope** of the liquidus curve, L, one could have either (a) penetration of the liquidus line, L, so that a thermodynamic free energy **driving force**, ΔG(t) for crystal growth **occurs** ($\dot{T}$ is much larger than $\dot{C}_A$) or it **doesn't** ($\dot{C}_A$ is much larger than $\dot{T}$).

For simplicity, let us assume that the evaporation rate is negligible and only $\dot{T}$ is important for us to consider for our description of the crystal volume formation process as a function of time. For even greater simplicity, let us consider that only **one** crystal nucleates at temperature $To - \left(\widehat{\Delta T} + \Delta T^*\right)$ and grows **spherically** at rate $\dot{R}$(t) (again for simplicity of communication). Figure 3 illustrates a typical plot of $\dot{R}(t)/R^*$, where R* is the critical nucleus formation size at supercooling below the liquidus line, L, of magnitude ΔT^* and R(t) is the actual crystal radius magnitude, via growth at time t.

To begin to discuss the coupled physical processes involved in any crystal growth event, we need to return to Figure 2 and recognize that the following must occur:

1. (a) The thermodynamic excess free energy of the liquid volume relative to the equivalent volume of solid, $\Delta G_F = G_L - G_S = \alpha \Delta T^*$ where α is approximately a constant for a particular material so that this growing thermodynamic driving force, $\Delta G = (\alpha \Delta \dot{T}^* + \dot{T}t)$ favors the formation of the solid nucleus.
   (b) However, when the solid nucleus forms, the interfacial area of the nucleus introduces an excess thermodynamic free energy to the nucleation process of γ per unit area of interface and this quantity hinders the formation of the solid nucleus.
   (c) Neglecting the fine details of the nucleation process, as ΔT^* increases with time, Factor (a) becomes larger than Factor (b) and the nucleation of a bit of solid does occur at some value of time, t*.

2. Next, at time T*, a solid sphere of Radius R*, is assumed to be present at the position (ΔT^*,$k_0 C_0$) below the liquidus line, L of Figure 2, where $k_0 C_0$ is the solidus concentration value at ΔT^* so that some of Solute B is partitioned into the adjacent liquid of the nucleus. This excess solute, (1-k_0)C_0, times the volume of the initial nucleus begins to diffuse into the bulk liquid at a rate determined by the matter transport process in the liquid. In turn, the liquid concentration of B seeks to be at the liquidus concentration value for that undercooling ΔT^*.

3. This matter transport of B begins to thermodynamically drive the actual crystal grow of the solid particle of radius R* so that latent heat begins to be released at the growing interface of the crystal. This, in turn, requires that the actual interface temperature, T$_i$, must be above the far-field temperature given by the supercooling, ΔT^*, in order for this latent heat to be conducted away from this growing solid.

4. These three simultaneous, **microscopic** processes of (a) interface creation, (b) matter transport and (c) heat transport during the crystal's growth in radius size demand the addition of a fourth **microscopic** process of atomic exchange of atoms A and B, from the average liquid thermodynamic free energy state to the solid crystal crystal thermodynamic free energy state.

5. Thus, overall, in any crystal growth process, the thermodynamic free energy driving process for change, ΔG, must be simultaneously partitioned into four parts, (1) excess energy storage in interfacial area growth with time, ΔG_γ, (2) microscopic interface kinetics of atomic state change, ΔG_K, (3) macroscopic heat transport to drive the crystal growth rate at $\dot{R}$, ΔG_T, and (4) macroscopic matter transport to drive the crystal growth rate with the interface being at the solidus and liquidus conditions, ΔG_S.

Pursuing a mathematically quantitative constraint on this overall process yields

$$\Delta G = \Delta G_\gamma + \Delta G_K + \Delta G_T + \Delta G_S \qquad (1)$$

which, in turn, yields a solution for $\dot{R}(t)$ (as in Figure 3) plus a determination of the **most stable** crystal interface morphology condition during crystal growth. In actual practice, this particular Figure 1b system analysis allowed our world to routinely grow the extremely high quality silicon single crystals[1] needed for today's solid state electronics revolution.

B. Oswald's rule for geological material phase transformations

In the foregoing section, a somewhat brief and idealized situation[1] has been utilized. In this section, I wish to jump to a more complex example to illustrate possible competitive factors that sometimes occur in **solid-sate** phase transformations that appear in nature.

Although ternary and quaternary, etc, phase diagrams can exist for specific elements or specific compounds (oxides, **sulphides**, etc) that can alloy together to form new species. Figure 4 is a fictitious binary, elemental phase diagram of atoms A and B that can be utilized to illustrate the **kinetic principle** that I wish to unveil. Here, solids, B,C,D,E,F,G and H are different compounds of the form A_nB_m, where n and m are integers with values 1,2,3,4, etc. In Figure 4, T_E is called the eutectic temperature where solid A and Solid B (type Q) can simultaneously form. Let us presume that, at T_E, the system is suddenly quenched by an amount ΔT^*.
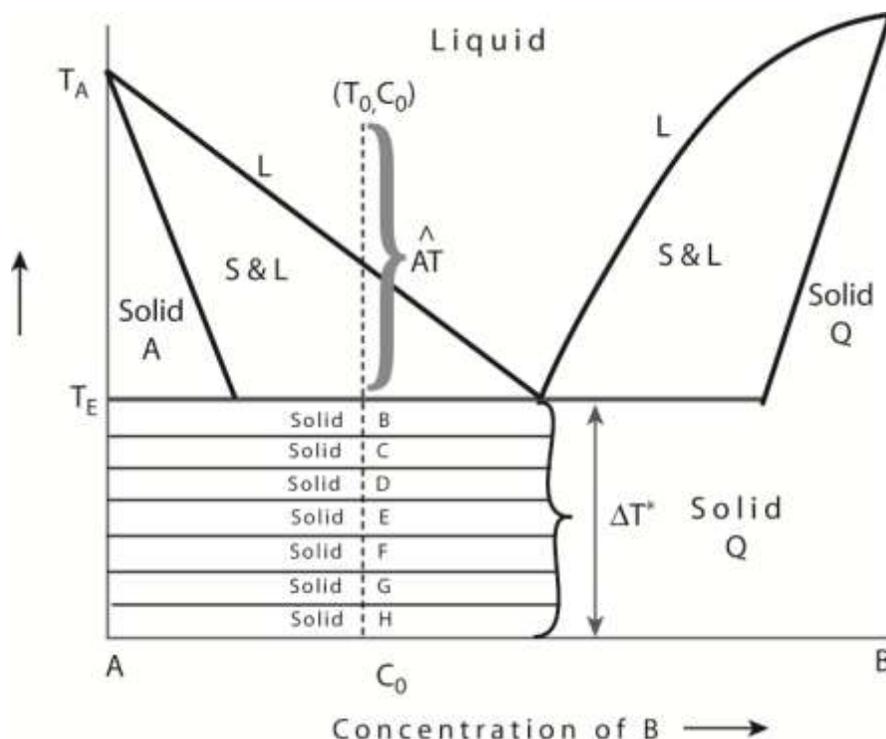
Figure 4. A more complex, but possible, binary phase diagram of elements A and B illustrating a significant array of thermodynamically stable solid phases on the A-rich side.

Now, B,C,D,E,F,G and H become thermodynamically stable with Phase H being the most stable of this set of solid phases. On the left side, the solid Phase A and the liquid at the eutectic concentration, C_E, (at temperature T_E) are now thermodynamically required to transform to another phase. This can easily occur on the right side of the diagram because it is a simple liquid to solid, Q, phase transformation. However, on the left side of the diagram, it is a solid to solid phase transformation, a **much, much** slower process **kinetically**, while **thermodynamically**, all of the A→B,C,D,E,F,G,H options are viable but with successively increased magnitude of thermodynamic driving force. Even if nuclei of all Phases B,C,D,E,F,G and H actually form initially, it is the **kinetically** fastest transforming phase of this group that first appears. Let us presume that it is solid phase C. Since this phase is thermodynamically unstable with respect to solid Phase D,E,F,G and H, this thermodynamic/kinetically dominant phase transformation process selects the next choice of sequential solid to solid phase formation until, eventually, the thermodynamic driving force is totally used up and the final, thermodynamically stable phase is H. This sequence of phase transformations is called "Ostwald's Rule" and is typical of many geological phase transformations in nature. Of course, this total process may take hundreds of thousands to millions of years!

The important and relevant point to gather from this example is that, although the thermodynamics drives the long-term process of change, it is the kinetics of change that determines the short-term process of transformation. Thus, this step by step, sequence of "unbuilding" the old structure by atom or molecule movements and "rebuilding" a new, more thermodynamically favorable structure (even if it is not the **most** favorable structure thermodynamically), it is the path that "nature" takes to bring about change to produce the most thermodynamically stable material possible (with a thermodynamic driving force for change of zero).

C. How ATEC and Zung monthly questionnaires act as time-varying thermodynamic driving forces, ΔG_C and ΔG_P, for transformational changes in child, ΔG_C and parent, ΔG_P, humans

From earlier work on Reconnective Healing[2], we were able to experimentally show that, when humans participated in such workshops and build **new information** into themselves, they automatically increased the level of coherence manifesting in the workshop room. In follow-on work, we were able to show that this actually altered the Gibb's thermodynamic free energy, G, of the space in a beneficial way[3].

The standard expression for G in today's world is

$$G = PV + E - T S_0 \tag{2a}$$

Where P=pressure, V=volume, E=internal energy, T=temperature and S_0 is entropy. This equation can also be written as

$$G = H - TS_0 \quad \text{and} \quad H = PV + E \tag{2b}$$

where H is the chemical enthalpy of the system. Simultaneous experimental measurement of both G(t) and T(t) as a function of time, t, allows one to take slopes of the two curves and yield $(\delta G/\delta t)_P$ and $(\delta T/\delta t)_P$ which, from equations 2b allows both S_0 and H to be determined as a function of time. Further, if an experiment is carried out wherein new information, ΔI, is created, information theory[4-6] tells us that

$$\Delta I = -\Delta S \tag{2c}$$

And that an exactly equivalent amount of negative entropy is created. Such a reduction of entropy in the system actually increases the value of G for the system, which can constitute a new thermodynamic driving force for change.

The foregoing means that, in an experiment where new information, $\Delta I(t)$, is created, the Gibb's thermodynamic free energy equation becomes

$$G = PV + E - T\left(S_0 + \int_{t_1}^{t_2}(\delta S(t) + \delta I(t))dt\right) \tag{2d}$$

where $\delta S(t)$ is the incremental positive entropy cost to create the incremental new information change, $\delta I(t)$. Integrating Equation 2d over the time period, T_2-T_1, allows one to determine if a net **negentropy** contribution in nature has been created by the particular experiment. For the particular Reconnection Healing experiment being investigated, Figure 5 provides examples of the bracketed term in Equation 2d for various stages during the workshop event. One can see that the maximum negative entropy production period occurred during lunch time when the room was quietly used for private healing sessions!
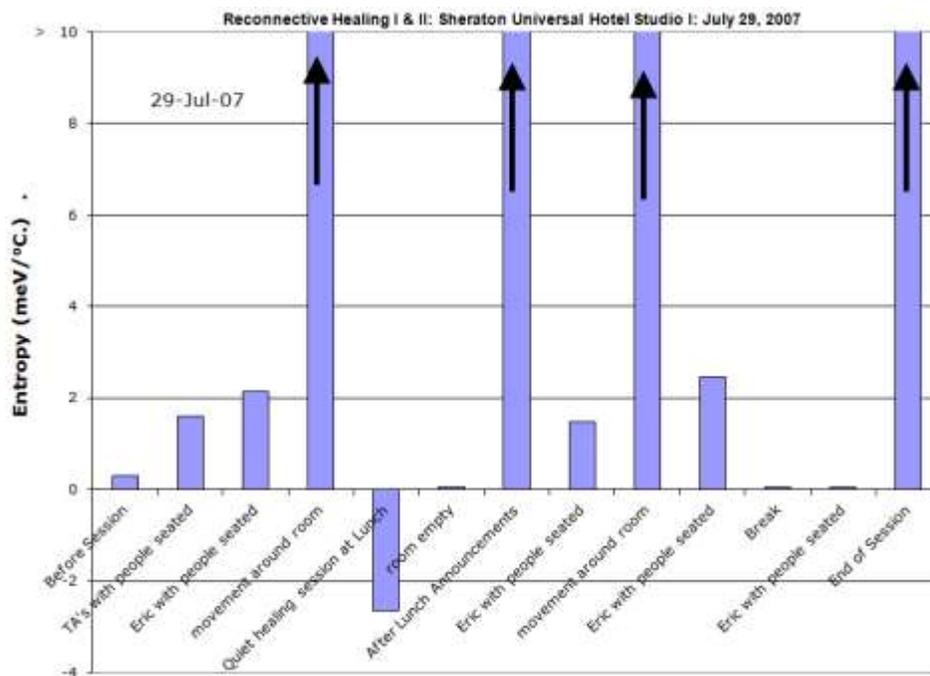

Figure 5. Total entropy reaction vs. time for a Reconnective Healing Workshop.

Perhaps the most important consequence of this section to note is that the psychological questionnaires utilized in each of our global IHD broadcasting experiments has catalogued new information creation events in nature. Thus, these plots actually represent changes in negentropy or, equivalently, positive "ΔG" changes in standard thermodynamic free energy fashion.

With this new perspective, the Figure 1 procedure can be applied to the global Autism Broadcasting experiment with IHDs providing the "IS" for the two human systems of parents and their autistic children while the new information created via the Zung and ATEC 12-monthly plots represent "OR"-responses of a thermodynamic ΔG_Z and ΔG_A nature, respectively. In both cases we gain some perspective on how we might begin to hypothesize some internal structural features of the "black

boxes" for example: from my earlier writings, I proposed the three selves model illustrated in Figure 6 and the various categories of substance/energies illustrated in Figure 7.
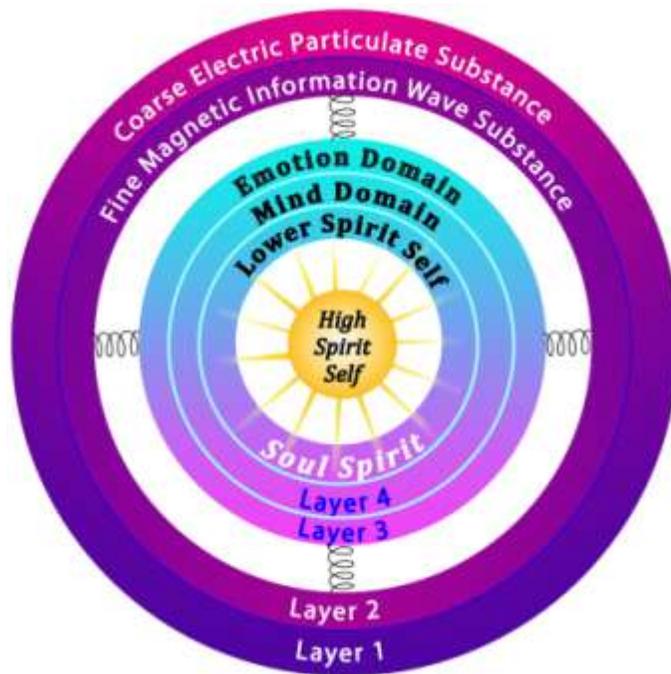

Figure 6. I like to visualize a sphere comprised of three concentric zones that are at least weakly coupled to each other. The outermost two layers is the personality self. The middle three layers is the soul self. The core region is the high spirit self (or the God Self).
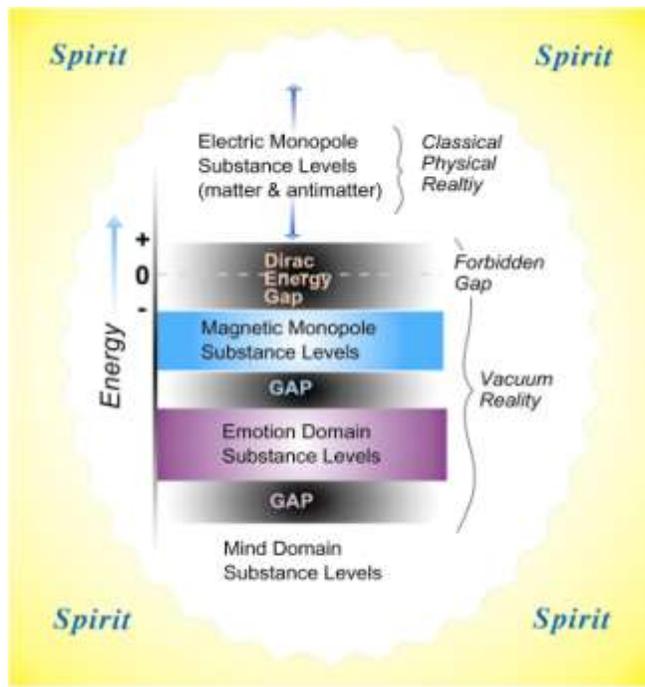
Figure 7. An energy level diagram embracing both classical physical substances and "unseen" vacuum substances.
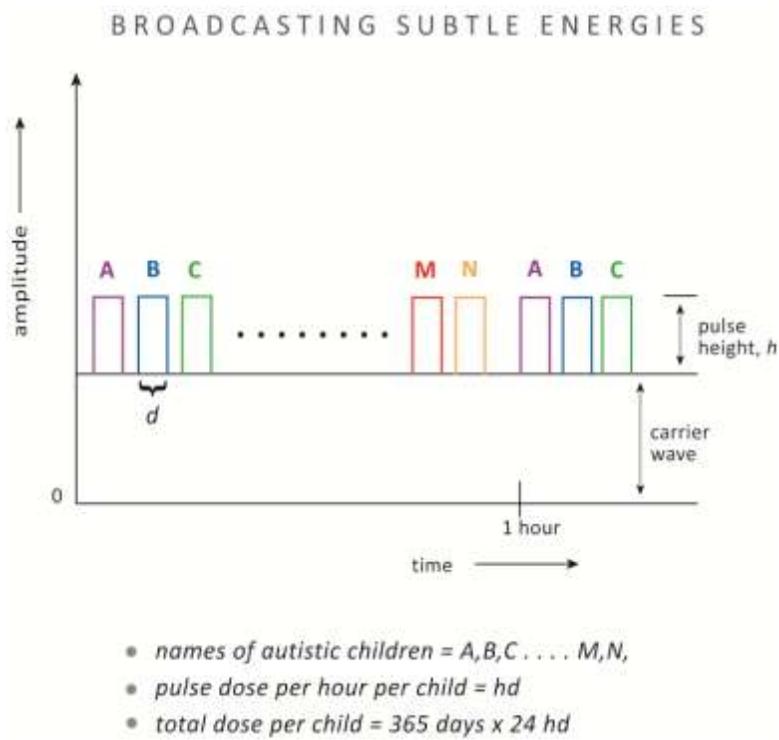

Figure 8. Subtle energy broadcast pattern for continuous broadcasting to autism parents and children at their global postal address.

Here, our IHDs can produce significant changes as a hypothetical platform for the production of beneficial changes in humans utilizing the working hypothesis model of

$$\Delta G = \Delta G_e + \Delta G_m + \Delta G_E + \Delta G_M + \Delta G_S \, . \qquad\qquad (3)$$

This utilizes the specific intention imbedded into our IHD as the thermodynamic "IS" driving force for information, energetic, structural and chemical changes in our human "black box". This is realized by the altered "OR" in the form of Zung and ATEC questionnaire response plots.

As practical tools in such a study, we presently can (1) alter the specific details of the imprint statement imbedded into the IHD and (2) alter the specific details of the broadcast profile illustrated in the figure of Appendix I of White Paper XXXI and given here as Figure 8. Currently, we are intending to reduce the broadcast intensity by a factor of two for the children participants to hopefully (a) reduce any transformational stresses for the children and (b) cause the parent, child correlation coefficients, $\Delta P/\Delta C_j$, to be increased to unity for all four child skill sets.

References

1. W.A. Tiller, The Science of Crystallization: Microscopic Interfacial Phenomena, Chapter 1, (Cambridge University Press, Cambridge (U.K.), New York (USA), etc, 1991).
2. W.A. Tiller and W.E. Dibble, Jr., White Paper #XI, online document at www.tiller.org.
3. W.A. Tiller and W.E. Dibble, Jr., White Paper #XXXIV, online document at www.tiller.org.
4. C.E. Shannon, "A mathematical theory of communication", The Bell System Technical Journal, 27, 379-423 (July) and 623-656 (October).
5. C.E. Shannon and W. Weaver, The Mathematical Theory of Communication (University of Illinois Press, Urbana, Illinois, 1949).
6. L. Brillouin, Science and Information Theory, Second Addition (Academic Press, New York, NY, 1952).